A genetically inducible endothelial niche enables vascularization of human kidney organoids with multilineage maturation and emergence of renin expressing cells

see commentary on page 1017

OPEN

Joseph C. Maggiore[1,2], Ryan LeGraw[3,4], Aneta Przepiorski[1], Jeremy Velazquez[3,4], Christopher Chaney[5,6,7], Thitinee Vanichapol[8], Evan Streeter[1,2], Zainab Almuallim[1,2], Akira Oda[9], Takuto Chiba[9], Anne Silva-Barbosa[9], Jonathan Franks[10], Joshua Hislop[4,11], Alex Hill[3,4], Haojia Wu[12], Katherine Pfister[9], Sara E. Howden[13], Simon C. Watkins[10], Melissa H. Little[13,14,15], Benjamin D. Humphreys[12,16], Samira Kiani[3,4,10,17], Alan Watson[10], Donna B. Stolz[10], Alan J. Davidson[8], Tom Carroll[5,6,7], Ondine Cleaver[5], Sunder Sims-Lucas[9], Mo R. Ebrahimkhani[3,4,5,11] and Neil A. Hukriede[1,2]

[1]Department of Cell Biology, School of Medicine, University of Pittsburgh, Pittsburgh, Pennsylvania, USA; [2]Center for Integrative Organ Systems, University of Pittsburgh, Pittsburgh, Pennsylvania, USA; [3]Department of Pathology, Division of Experimental Pathology, School of Medicine, University of Pittsburgh, Pittsburgh, Pennsylvania, USA; [4]Pittsburgh Liver Research Center, University of Pittsburgh, Pittsburgh, Pennsylvania, USA; [5]Department of Molecular Biology, University of Texas Southwestern Medical Center, Dallas, Texas, USA; [6]Hamon Center for Regenerative Science and Medicine, University of Texas Southwestern Medical Center, Dallas, Texas, USA; [7]Department of Internal Medicine, Division of Nephrology, University of Texas Southwestern Medical Center, Dallas, Texas, USA; [8]Department of Molecular Medicine and Pathology, University of Auckland, Auckland, New Zealand; [9]Department of Pediatrics, School of Medicine, University of Pittsburgh, Pittsburgh Pennsylvania, USA; [10]Center for Biologic Imaging, University of Pittsburgh, Pittsburgh, Pennsylvania, USA; [11]Department of Bioengineering, Swanson School of Engineering, University of Pittsburgh, Pittsburgh, Pennsylvania, USA; [12]Division of Nephrology, Department of Medicine, School of Medicine, Washington University in St. Louis, St. Louis, Missouri, USA; [13]Murdoch Children's Research Institute, Melbourne, Victoria, Australia; [14]Department of Anatomy and Neuroscience, The University of Melbourne, Melbourne, Victoria, Australia; [15]Department of Paediatrics, The University of Melbourne, Melbourne, Victoria, Australia; [16]Department of Developmental Biology, School of Medicine, Washington University in St. Louis, St. Louis, Missouri, USA; and [17]McGowan Institute for Regenerative Medicine, University of Pittsburgh, Pittsburgh, Pennsylvania, USA

Vascularization plays a critical role in organ maturation and cell-type development. Drug discovery, organ mimicry, and ultimately transplantation hinge on achieving robust vascularization of *in vitro* engineered organs. Here, focusing on human kidney organoids, we overcame this hurdle by combining a human induced pluripotent stem cell (iPSC) line containing an inducible ETS translocation variant 2 (ETV2) (a transcription factor playing a role in endothelial cell development) that directs endothelial differentiation *in vitro*, with a non-transgenic iPSC line in suspension organoid culture. The resulting human kidney organoids show extensive endothelialization with a cellular identity most closely related to human kidney endothelia. Endothelialized kidney organoids also show increased maturation of nephron structures, an associated fenestrated endothelium with *de novo* formation of glomerular and venous subtypes, and the emergence of drug-responsive renin expressing cells. The creation of an engineered vascular niche capable of improving kidney organoid maturation and cell type complexity is a significant step forward in the path to clinical translation. Thus, incorporation of an engineered endothelial niche into a previously published kidney organoid protocol allowed the orthogonal differentiation of endothelial and parenchymal cell types, demonstrating the potential for applicability to other basic and translational organoid studies.

Correspondence: *Mo R. Ebrahimkhani, Department of Pathology, University of Pittsburg, 3501 5th Avenue, 5061 BST3, Pittsburgh, Pennsylvania 15213, USA; E-mail: mo.ebr@pitt.edu; or Neil A. Hukriede, Department of Cell Biology, University of Pittsburg, 3501 5th Avenue, 5061 BST3, Pittsburgh, Pennsylvania 15213, USA. E-mail: hukriede@pitt.edu*

Received 1 September 2023; revised 10 May 2024; accepted 24 May 2024; published online 18 June 2024

Kidney International (2024) **106,** 1086–1100; https://doi.org/10.1016/j.kint.2024.05.026

KEYWORDS: endothelial; genetic engineering; organoids; podocytes; renin; scRNAseq

Engineering clinically relevant microphysiological tissues *in vitro* hinges on the codevelopment of a robust endothelial network. Although endothelial cells play an important role in forming the vessels that transport blood and nutrients, they also interact with developing tissues and promote maturation.[1–7] Furthermore, across most organ systems, the vasculature plays a crucial role in disease processes. Therefore, *in vitro* organ models that lack the

Translational Statement

Development of therapies for patients with kidney diseases relies on a morphologically and physiologically representative *in vitro* model. Human kidney organoids are an attractive model to recapitulate kidney physiology, but they are limited by the absence of a vascular network and mature cell populations. In this work, we have generated a genetically inducible endothelial niche that, when combined with an established kidney organoid protocol, produces a robust endothelial cell network, promotes podocyte maturation, and induces the emergence of a functional renin cell population. This advance significantly increases the clinical relevance of human kidney organoids for etiologic studies of kidney disease and future regenerative medicine strategies.

endothelial niche are limited in their capacity to recapitulate native physiology and model disease. Methods for vascularizing *in vitro* organ systems have been developed with varying levels of success; these have included bioprinting vasculature,[8] inducing vasculature using flow systems,[9] and supplementing cell-culture systems with proteins or transcription factors.[10] One of the key cell types in the vasculature is the endothelial lining, which studies have attempted to reconstruct *in vitro* through transgenic induction of an orthogonal hemato-endothelial population of cells.[11–15] This approach is particularly attractive, given that it both bypasses a hurdle in developing a common universal culture media to coax the generation of heterogenous cell types and allows for orthogonal differentiation of the parenchymal tissue of interest.

Recapitulating vasculature in *in vitro* kidney systems proves no less challenging. Kidney vasculature regulates blood pressure, controls filtration of serum ions and proteins, and regulates many important endocrine pathways[16]; thus, it is critically important to model for studies of kidney physiological health. Similarly, in disease settings, endothelial cells can become inflamed, apoptose, and/or fibrose, ultimately contributing greatly to a patient's disease burden across many kidney diseases.[17,18] Current methods for vascularizing the *in vitro* human kidney constructs[19] have followed methods similar to those used for other organ systems, including flow enhancement with chips,[20–22] decellularizing and/or recellularizing extracellular matrix,[23] bioprinting,[24] renal subcapsular transplantation,[25,26] vascular endothelial growth factor (VEGF) supplementation,[27] and time-dependent modulation of WNT1 (Wnt family member 1) and fibroblast growth factor 9 (FGF9).[28] However, these methods still leave multiple unmet needs.[29] Notably, a critical requirement is a method of vascularization that can do the following: (i) reliably and simply generate a network that integrates with the kidney parenchyma in 3 dimensions; (ii) allow for orthogonal differentiation and codevelopment of endothelial and non-endothelial cell types; (iii) be applied broadly to multiple existing kidney tissue–engineering protocols; (iv) be highly reproducible, thereby minimizing batch-to-batch variation; (v) be applicable in settings of high throughput kidney physiology and disease modelling; and (vi) not require usage of expensive supplemented growth factors.

For these reasons, we turned to *ETS translocation variant 2* (*ETV2*), which previously was shown to play a central role in directing endothelial cell differentiation.[30,31] We developed an engineered inducible ETV2-human induced pluripotent stem cell line (iETV2-hiPSC). Previous publications have engineered ETV2-expressing cells to vascularize human cortical organoids[15] and neural tissue[14]; however, iETV2-hiPSCs have not been utilized to vascularize human kidney organoids. Here, we incorporated iETV2-hiPSCs into a previously established human kidney organoid bioreactor protocol,[32,33] to reconstitute an endothelial niche in tandem with *in vitro* kidney organogenesis. We show that the resulting endothelial niche contains fenestrated kidney endothelial subtypes, improves the maturation of podocytes, induces the formation of a renin$^+$ cells, and results in significant cell–cell interactions between endothelial and parenchymal cells.

METHODS

Generating inducible ETV2 hiPSCs

Reverse tetracycline-controlled transactivator (rtTA) expressing Personal Genome Project (PGP)1 hiPSCs previously generated[34] were transfected, as we and other groups have done,[30,35,36] using Lipofectamine 3000 (Thermo Fisher Scientific, L3000001) with Super PiggyBac Transposase (System Biosciences, PB210PA-1) and the PiggyBac transposon vector with hETV2-2A-enhanced green fluorescent protein (EGFP) under control of the tetracycline responsive element promoter. Transfected cells were selected by adding 0.5 mg/ml puromycin to mTeSR1 maintenance medium (STEMCELL Technologies, 85850). PGP1-ETV2 hiPSCs were karyotyped using Thermo Fischer Scientific Karyostat+ Karyotyping service.

Cell-culture and kidney-organoid generation

Kidney organoids were generated using the previously published MANZ2-2 hiPSC line[37] and the HNF4A-GATA3-MAFB (Triple) hiPSC line (Supplementary Methods, Supplementary Table S4). These cells were combined with PGP1-ETV2 hiPSCs to generate vascularized human kidney organoids. Kidney organoids were generated using a previously published protocol.[32,33] To generate vascularized kidney organoids, the PGP1-ETV2 hiPSC line was combined with a control hiPSC line (MANZ2-2 or Triple) at a ratio of 1:5 on day 0 in stage I media. The same protocol for organoid formation was carried out, with the addition of 0.5 mg/ml of doxycycline to stage II media from day 5 to day 18, supplemented each day, unless otherwise stated.

Whole mount clearing, immunofluorescence, and imaging

Organoids were fixed in 4% paraformaldehydes (PFAs; Fisher Scientific, AC416785000) for 24 hours and then rinsed in phosphate buffered saline (PBS) 3 times. Organoids then were rendered optically clear through an adapted

version of the Clear, Unobstructed Body Imaging Cocktail(s) and computational-analysis (CUBIC) clearing protocol[38–40] and immunolabelled with primary and secondary antibodies (Supplementary Methods, Supplementary Tables S1 and S2). Organoids then were imaged on a Nikon A1R Spectral Confocal microscope. Three-dimensional renderings of the organoids then were generated using Bitplane Imaris version 10.0.0 (Oxford Instruments). Images then were quantified to analyze vascular network and per-cell immunofluorescence, as described in the Supplementary Methods. Electron microscopy also was carried out on control and vascularized kidney organoids, with methods described in detail in the Supplementary Methods.

RNA extraction and reverse transcription quantitative polymerase chain reaction

RNA was extracted from monolayers of hiPSCs or whole kidney organoids using TRI Reagent (Thermo Fisher Scientific, AM9738) at room temperature for 30 minutes, with intermittent agitation. RNA isolation, cDNA synthesis, reverse transcription quantitative polymerase chain reaction, and downstream analysis were carried out using supplier-manufactured kits and are described in detail in the Supplementary Methods, and RT-qPCR primers can be found in Supplementary Table S3.

Single-cell (sc) and single-nuclear (sn) RNA sequencing (RNAseq) of ETV2-hiPSC line

For scRNAseq, iETV2-hiPSCs were prepared as described by the 10x Genomics Single Cell 3′ v2 Reagent Kit user guide. After 4 days of doxycycline exposure, a monolayer of cells was incubated with trypsin for 10 minutes at 37 °C, followed by gentle pipetting using a serologic pipette to dislodge and dissociate aggregates. Downstream scRNAseq then was carried out following 10X manufacturing guidelines, the details of which are described in the Supplementary Methods. For single-nuclear RNA sequencing of kidney organoids, day 18 MANZ2-2 control, and vascularized kidney organoids were washed in Dulbecco's (D) PBS once, then transferred into 37 °C 0.25% trypsin- ethylenediamine tetraacetic acid (EDTA; Gibco, 15400054) and incubated with intermittent agitation for 10 minutes to obtain single cells. Cells then were centrifuged at 800 rpm for 5 minutes and resuspended in DPBS and filtered through a 40-mm cell filter (pluriSelect, 43-50040-51). 10X protocol guidelines then were followed to carry out snRNAseq, the details of which are described in the Supplementary Methods, and recipes for solutions are found in Supplementary Tables S5–S7.

RESULTS

iETV2-hiPSCs generate endothelial cells following doxycycline exposure

We developed a doxycycline-inducible ETV2-EGFP hiPSC line (Supplementary Figure S1) that, when stimulated, generates a population of endothelial progenitor-like cells (Figure 1a). In monolayer iPSC culture, following a 24-hour doxycycline exposure, a marked induction occurred in immunofluorescence of ETV2-EGFP that persisted until day 2. Beginning at day 3 and lasting until day 6, with subsequent continued doxycycline exposure, an increase occurred in the immunofluorescence intensity of melanoma cell adhesion molecule 1 (MCAM) and platelet and endothelial cell adhesion molecule 1 (PECAM1) labeling (Figure 1b and c; Supplementary Figure S2). Subsequently, MCAM and PECAM1 reach peak immunofluorescence expression levels by day 7, which was confirmed by per-cell fluorescence intensity quantification (Figure 1b and c; Supplementary Figure S3).

To determine the transcriptomic identify of the induced cells, scRNAseq was performed on iETV2-hiPSCs exposed to doxycycline for 4 days (Figure 1d). A total of 1839 cells were used in downstream scRNAseq analysis, and uniform manifold approximation and projection (UMAP) plots were generated wherein 3 distinct cell clusters were identified (early endothelial-like progenitor population [P1], mid–endothelial-like progenitor cells [P2], late endothelial-like progenitor cells [P3]; Figure 1e). As identified using Monocle3 (Trapnell Lab),[41,42] a developmental trajectory was identified progressing from P1 → P2 → P3 (Figure 1f). These clusters contained transcriptional profiles similar to early, mid–, and late endothelial progenitor populations (Figure 1g). P1 was characterized by *ETV2*, *KLF4*, *GATA2*, and *RUNX1*; P2 cells were characterized by *ALCAM*, *TAL1*, and *MCAM*; and P3 cells were characterized by *PECAM1*, *FLT1*, and *CD34* (Figure 1g; Supplementary Figure S4).

To identify organ-specific or endothelial sublineage populations, transcriptomes of P1, P2, and P3 populations were compared with published human endothelial scRNAseq datasets from Tabula Sapiens,[43] using SingleCellNet (Cahan Lab).[44] The iETV2-hiPSC endothelial cells did not specifically align or express markers of organ-specific endothelial cell types (Supplementary Figure S5). Furthermore, these cells do not express high levels of *EFNB2* or *EPHB4*, which mark arteries and veins, respectively (Supplementary Figure S6). When the iETV2-hiPSCs were aligned against Tabula Sapiens endothelial cell gene ontology classifiers, alignment with terms indicative of endothelial-cell vascular tree morphology increased (Supplementary Figure S7). These data demonstrated that when cultured in monolayer, iETV2-hiPSCs generate a generic, organ-agnostic population of endothelial-like progenitor cells.

iETV2-hiPSCs form an integrated endothelial network in kidney organoids with maintained presence of critical parenchymal kidney cell types

We then modified an established kidney organoid protocol,[33,45,46] to include the integration of iETV2-hiPSCs (Figure 2a). Vascularized human kidney organoids were generated by combining a wild-type hiPSC (MANZ2-2 or Triple) line with the iETV2-hiPSC transgenic line. Both hiPSCs were scraped from monolayer culture, dissociated as clusters in suspension, and when combined, self-aggregated into spheroids, forming embryoid bodies by day 3. From culture day 5 to day 18, the organoids were exposed to doxycycline, inducing the transgenic

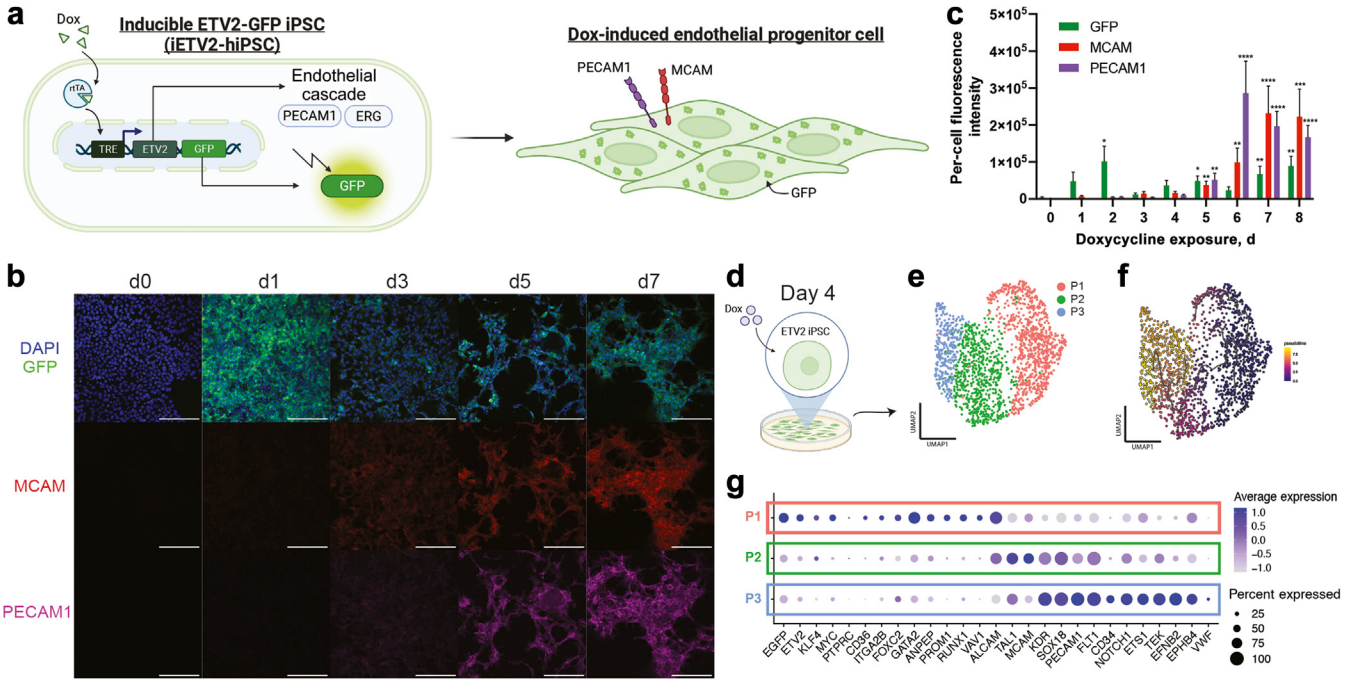

Figure 1 | Genetically inducible ETV2 human induced pluripotent stem cells (iETV2-hiPSCs) undergo synthetic endothelial differentiation. (**a**) Schematic of iETV2-hiPSC genetic circuit and path to differentiation. (**b**) iETV2-hiPSCs differentiated with doxycycline (dox) induction and representative immunofluorescent images from day 0 to day 9 from 3 biological replicates; bar = 200 um. (**c**) Per-cell immunofluorescent intensity quantification of green fluorescent protein (GFP), melanoma cell adhesion molecule 1 (MCAM), and platelet and endothelial cell adhesion molecule 1 (PECAM1) channels. N = 3 biological replicates; $^{****}P < 0.0001$, $^{***}P < 0.001$, $^{**}P < 0.01$, $^{*}P < 0.05$. (**d**) Graphical schematic of single-cell RNA sequencing (scRNAseq) carried out on iETV2-hiPSCs after they have been exposed to doxycycline for 4 days. (**e**) Uniform manifold approximation and projection (UMAP) of differentiated iETV2-hiPSCs generated 3 distinct cellular populations. (**f**) Pseudotime trajectory analysis with Monocle3 (Trapnell Lab) demonstrated developmental lineage from early endothelial-like progenitor population (P1) → mid–endothelial-like progenitor cells (P2) → late endothelial-like progenitor cells (P3). (**g**) Differentially expressed genes for P1, P2, P3. DAPI, 4′,6-diamidino-2-phenylindole; ERG, erythroblast transformation-specific-related gene; TRE, tetracycline responsive element. To optimize viewing of this image, please see the online version of this article at www.kidney-international.org.

iETV2-hiPSC line to differentiate into endothelial cells orthogonally from the wild-type iPSC line. The protocol was optimized for minimum effective doxycycline concentration, exposure window and length, and transgenic hiPSC-to–wild-type ratio, to yield a vascular network without compromising kidney organoid parenchymal cell types (Supplementary Figures S8 and S9). Independent of changing the ratio of cell types, a consistent number of $EGFP^{+}/PECAM1^{+}$ cells form, indicating a potential self-regulation of endothelial cell number (Supplementary Figure S10). We found that the ideal ratio to yield vascularized kidney organoids was a combination of 1:5 iETV2:wild-type hiPSCs, induced with 0.5 mg/ml doxycycline from day 5 to day 18 (Supplementary Figures S8–S10).

By day 18, a significant endothelial network had formed throughout the entire kidney organoid, as demonstrated by immunofluorescence of PECAM1 (Figure 2b), endomucin, and neuropilin 1 (NRP1; Supplementary Figure S11), and by reverse transcription quantitative polymerase chain reaction (Supplementary Figure S12). The endothelial network was analyzed with AngioTool[47] on immunofluorescent PECAM1 images showing an ∼2-fold increase in vessel area ($P < 0.0001$), an ∼2-fold increase in total vessel length ($P < 0.0001$), and an ∼3.60-fold increase in the number of junctions ($P < 0.0001$), compared to the values in controls (Figure 2c). Although the total number of starting cells for embryoid body formation was similar in the control versus vascularized conditions, the diameter of vascularized organoids was found to be ∼60% larger than that of the control organoid ($P < 0.0001$; Figure 2c).

To determine the stability of vessels generated within the organoids, we assessed whether they could connect with an *in vivo* blood supply. We implanted human kidney organoids with or without iETV2-hiPSCs under the kidney capsule of NOD scid gamma (NSG; Jackson Laboratory) mice as previously described,[25] and perfused them with a vascular tracer. These organoids were allowed to mature *in vivo* for either 21 (for tracer studies) or 28 (for stability studies) days. Vessels in organoids that did not contain the iETV2-hiPSCs were not perfused and were derived from the mouse as previously shown[25] (Supplementary Figure S13). Conversely, the iETV2-hiPSCs vascularized kidney organoids contained vessels that were perfused and stained positive for human GAPDH and human anti-nuclear antigen (ANA; Supplementary Figure S13). Overall, this data demonstrated that the addition of iETV2-hiPSCs generates a robust endothelial network

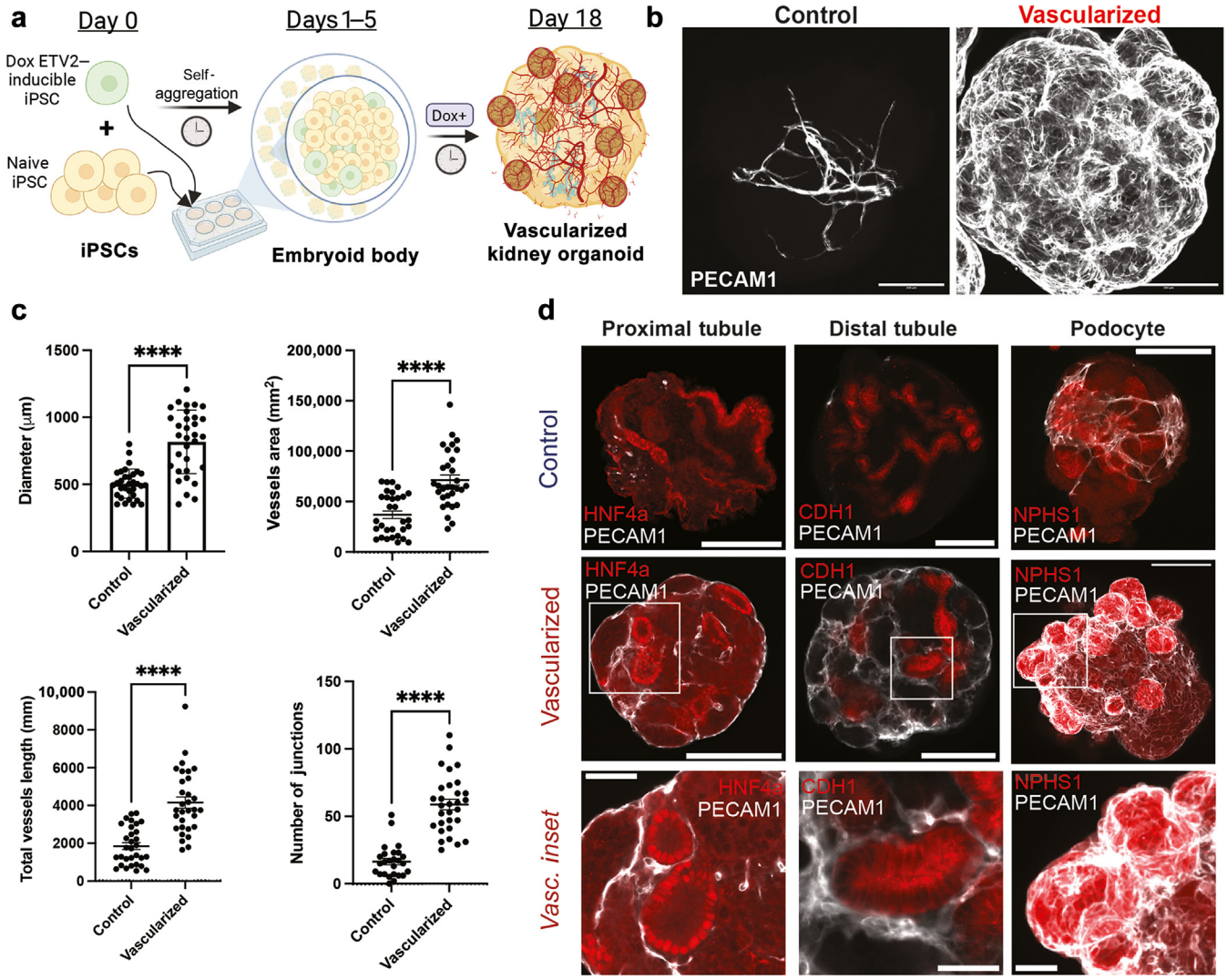

Figure 2 | Vascularization of human kidney organoids. (**a**) Method for vascularizing human kidney organoids by combining genetically inducible ETV2 human induced pluripotent stem cells (iETV2-hiPSCs) with wild-type iPSCs. (**b**) Representative immunofluorescent platelet and endothelial cell adhesion molecule 1 (PECAM1) images of endothelial cell network between the MANZ2-2 control and vascularized kidney organoids from 3 independent biological replicates. (**c**) AngioTool quantification and diameter measurement between control and vascularized kidney organoids; organoids from 3 biological replicates. ****$P < 0.0001$. (**d**) Representative immunofluorescence images of endothelial interaction with podocytes, proximal tubule, distal tubule, and stroma between control and vascularized (Vasc.) kidney organoid from 3 biological replicates. Organoid images, bar = 200 mm; inset bar = 50 mm. CDH1, cadherin-1; dox, doxycycline; HNF4A, hepatocyte nuclear factor 4 alpha; NPHS1, nephrin. To optimize viewing of this image, please see the online version of this article at www.kidney-international.org.

within the kidney organoid that can be sustained with an *in vivo* connection to a mouse host vasculature.

As has been shown utilizing this kidney-organoid protocol,[33,45,46] large nodules of nephrin+ (NPHS1$^+$) cells were evident at the cortex of the vascularized kidney organoids. With the addition of iETV2-hiPSCs, these clusters were seen to be enveloped by endothelial cells (Figure 2d), with occasional presence of endothelial cells contained within the NPSH1$^+$ cluster. Proximal and distal tubules, imaged in cross-section, appear to be encased in endothelial cells, which was not observed in the MANZ2-2 control kidney organoids (Figure 2d). However, we did not notice differences in the morphology of epithelial cells (Figure 2d).

To understand how organoid cellular composition changes upon vascularization, snRNAseq was carried out on day-18 MANZ2-2 control and vascularized kidney organoids (Figure 3a). On UMAP, cells from control and vascularized kidney organoid (Figure 3b) clustered by distinct cell types—podocytes, proximal nephron, distal nephron, endothelial cells, and interstitial cells (Figure 3c)—and expressed characteristic cell-type specific markers (Figure 3d), as confirmed using DevKidCC[48] (Supplementary Figure S14). The endothelial population (966 cells) was comprised of mostly endothelial cells from the vascularized kidney organoid (888 cells; 91.9%), and nearly all *EGFP* expression was localized to the endothelial

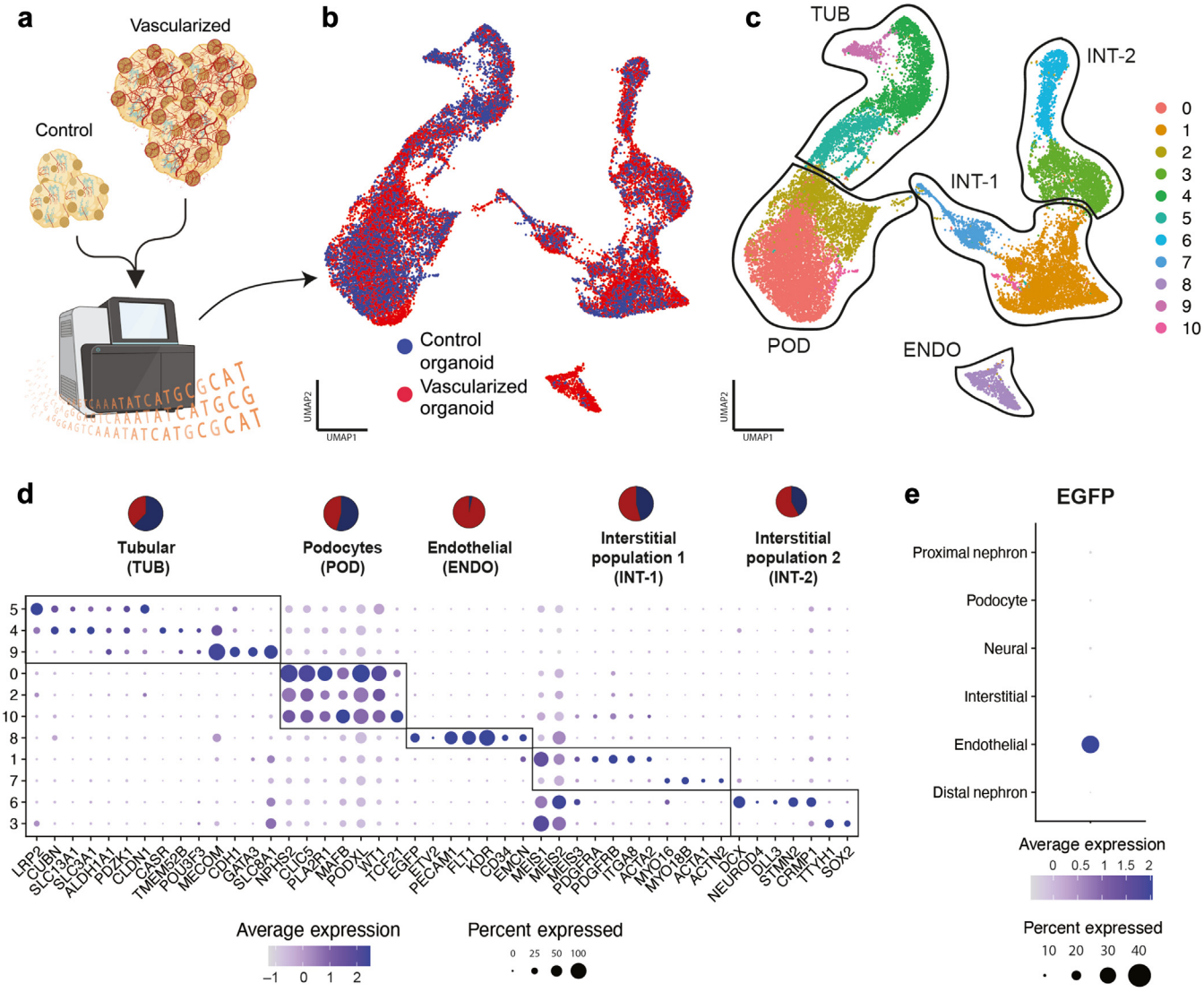

Figure 3 | Single-nuclei RNA sequencing (snRNAseq) of control and vascularized human kidney organoids. (**a**) Graphical schematic demonstrating MANZ2-2 control and vascularized human kidney organoids analyzed via snRNAseq. (**b**) Cells from control and vascularized kidney organoid aggregated and were well overlapped on uniform manifold approximation and projection (UMAP). (**c**) Cells on UMAP clustered by cell type as podocyte (POD), endothelial (ENDO), tubular (TUB), and interstitial (INT-1/2). (**d**) Differentially expressed genes per cluster were identified with dot plot. Cellular populations were quantified to analyze composition by control or vascularization origin and graphed as pie chart per cell type (red = vascularized; blue = control). (**e**) Feature dot plot demonstrated enhanced green fluorescent protein (EGFP) expression was localized to the endothelial population.

population (Figure 3e). The total organoid endothelial cell percentage for the control kidney organoid was 0.61%, compared to 6.9% under vascularized conditions. Podocyte (POD) and interstitial cluster 1 (INT-1) populations contained populations that were distributed evenly between control and vascularized kidney organoid cells (54.4% and 45.6%, respectively; Figure 3d). Tubular segments contained a slightly higher percentage of cells in the control kidney organoid (23.5% vs. 14.3%), whereas interstitial cluster 2 (INT-2) was comprised of cells in slightly greater proportions compared to vascularized kidney organoids (18.6% vs. 13.2%; Figure 3d). Cells of the tubular cluster, which further subclustered into proximal and distal tubule cells, did not show significant expression differences between the control and vascularized conditions (Supplementary Figure S15). The control and vascularized kidney organoid populations then were compared with scRNAseq datasets from previously published protocols. The organoids generated from the Takasato protocol[49] contained a similar proportion of endothelial cells (8.75%) as the vascularized kidney organoid (6.92%); however, the organoids from the Takasato protocol contained a smaller proportion of tubular cells and podocytes (13.29%) than did the vascularized kidney organoid (47.78%; Supplementary Figure S16A–C). The organoids generated from the Morizane protocol[50–52] contained a proportion of parenchymal and stromal cells similar to that in the control

and vascularized kidney organoids. However, the organoids generated from the Morizane protocol lacked a robust population of endothelial cells (0.26%) compared to vascularized organoids (6.92%; Supplementary Figure S16D–F). Cell populations from the Morizane protocol and Takasato protocols both overlapped in classical cell-type specific markers with the control and vascularized kidney organoids (Supplementary Figure S16F and G).

To examine whether the control and vascularized kidney organoid cell types correlated with cell types of *in vivo* human kidneys, we combined the organoid datasets with previously published, week 11–18 human fetal kidney scRNAseq datasets.[53] Cells from our kidney organoid populations overlapped well with human fetal kidney populations and were separated into distinct cell-type populations on combined UMAP (Supplementary Figure S17A and B). Although many of the cell types, such as proximal tubule and distal tubule, overlapped similarly with canonical key cell-type transcription markers, the fetal kidney and the organoids contained distinct and separate stromal populations that did not overlap (Supplementary Figure S17C). Additionally, the fetal human kidney contained a nephron progenitor-cell population that the organoids did not (Supplementary Figure S17B). Finally, podocytes in control and vascularized kidney organoids contained higher expression levels of mature podocyte markers, such as *NPHS1*, *NPHS2*, *PLCE1,* and *PTPRO,* than the human fetal kidney (Supplementary Figure S17C).

Vascularized kidney organoid enables greater differentiation of podocytes and improved endothelial cell–cell interaction

Podocytes have a highly specialized morphology consisting of interdigitating foot processes, and they associate closely with endothelial cells with a glomerular basement membrane (GBM) in-between.[54] Modeling podocyte–endothelial interaction is necessary to adequately understand mechanisms of glomerular filtration or identify therapeutics for podocytopathies.[55,56] Podocyte-like cells are present in MANZ2-2 control organoids; however, they generally have little to no endothelial cell integration, foot process development, or GBM[29,57] (Figure 4a; Supplementary Figure S18A). We found that NPHS1$^+$ podocytes in MANZ2-2 control kidney organoids exist as a defined cluster of cells on the exterior surface of the kidney organoid, with microvilli projections (Supplementary Figure S19A and B). The podocytes contain numerous protrusions, possibly representing primitive foot processes, which extend out from the exterior surface randomly or contact similar protrusions from other podocytes (Supplementary Figure S19C).

By contrast, vascularized kidney organoids contained an extensive EGFP$^+$/PECAM1$^+$ endothelial-cell network that interacts with the NPHS1$^+$ podocyte clusters (Figure 4a and b; Supplementary Figure S18B). In developing organoids from days 6–10, the EGFP$^+$ cells existed as distinct cell populations adjacent to other parenchymal cell populations, including Wilms' tumor 1 (WT1)$^+$ podocyte progenitor cells, but they are not intermixed. However, by days 14–18, the EGFP$^+$ cells appeared within distinct WT1$^+$ podocyte clusters, and by day 18, they display increased PECAM1 expression within the podocyte cluster (Supplementary Figure S18B). The endothelial cells encased the podocyte clusters, as seen by SEM (Supplementary Figure S19D and E), and on immunogold transmission electron microscopy, they are found to abut one another (Supplementary Figure S19F). These data demonstrate that the iETV2-hiPSCs do not exist in isolation as an endothelial cluster, but instead directly interact with podocytes.

To better interrogate whether iETV2-hiPSC organoids drive podocyte maturation, snRNAseq podocytes from control and vascularized kidney organoids were separated into 2 distinct clusters on UMAP (Figure 4c and d). Cluster 1 was comprised largely of podocytes from the vascularized kidney organoid (74.1%), whereas cluster 0 was comprised largely of podocytes from the control kidney organoid (60.5%; Figure 4e). Prior studies of podocytes in human fetal kidney transcriptomics found 2 populations of podocytes with distinct gene expression patterns—early podocytes (*OLFM3*, *GFRA3*, *PAX8*, *LHX1*, *PCDH9*) and late podocytes (*CLIC5*, *PLCE1*, *PTPRO*, *NPHS1*, *NPHS2*).[53,58] We find podocytes in both MANZ2-2 control and vascularized kidney organoids contain higher levels of late markers than early markers (Supplementary Figure S20).

Podocytes in the vascularized kidney organoid contain higher expression levels for markers of slit diaphragm and basement membrane formation, such as *SLIT2*, *SLIT3*, *NID2*, *COL4A1*, *COL4A2*, and *LAMB1* (Figure 4f). Furthermore, a gene ontology search was conducted for the top 100 differential expressed genes from the vascularized podocyte predominant cluster, which resulted in a marked increase in gene ontology matches for GBM formation, glomerular development, endothelial vascular differentiation and migration, and tight junction regulation (Figure 4g; Supplementary Figure S21). Previous studies have described the maturation of podocyte basement membrane composition by an isotype transition of COL4A1/2 to COL4A3/4/5 and a transition in laminins from LAMA1 to LAMC1 to LAMA5.[56,59] We found that podocytes of the vascularized kidney organoid contained higher proportions of mature basement markers than the control podocytes, such as *COL4A5*, *LAMC1*, and *LAMA5* (Supplementary Figure S20B). Additionally, we found that podocytes in vascularized kidney organoids have a fine plasma membrane localization of COL4A5 by immunofluorescence, whereas podocytes in the nonvascularized control kidney organoids do not show this interlaced staining (Supplementary Figure S20C). Finally, in comparing podocytes of control and vascularized kidney organoid origin to podocytes from Morizane and Takasato organoid-derived podocytes (Supplementary Figure S16I), we find upregulation of markers of basement membrane formation and glomerular development (Supplementary Figure S16J).

To determine cell–cell communication between podocytes and endothelial cells, scRNAseq populations were

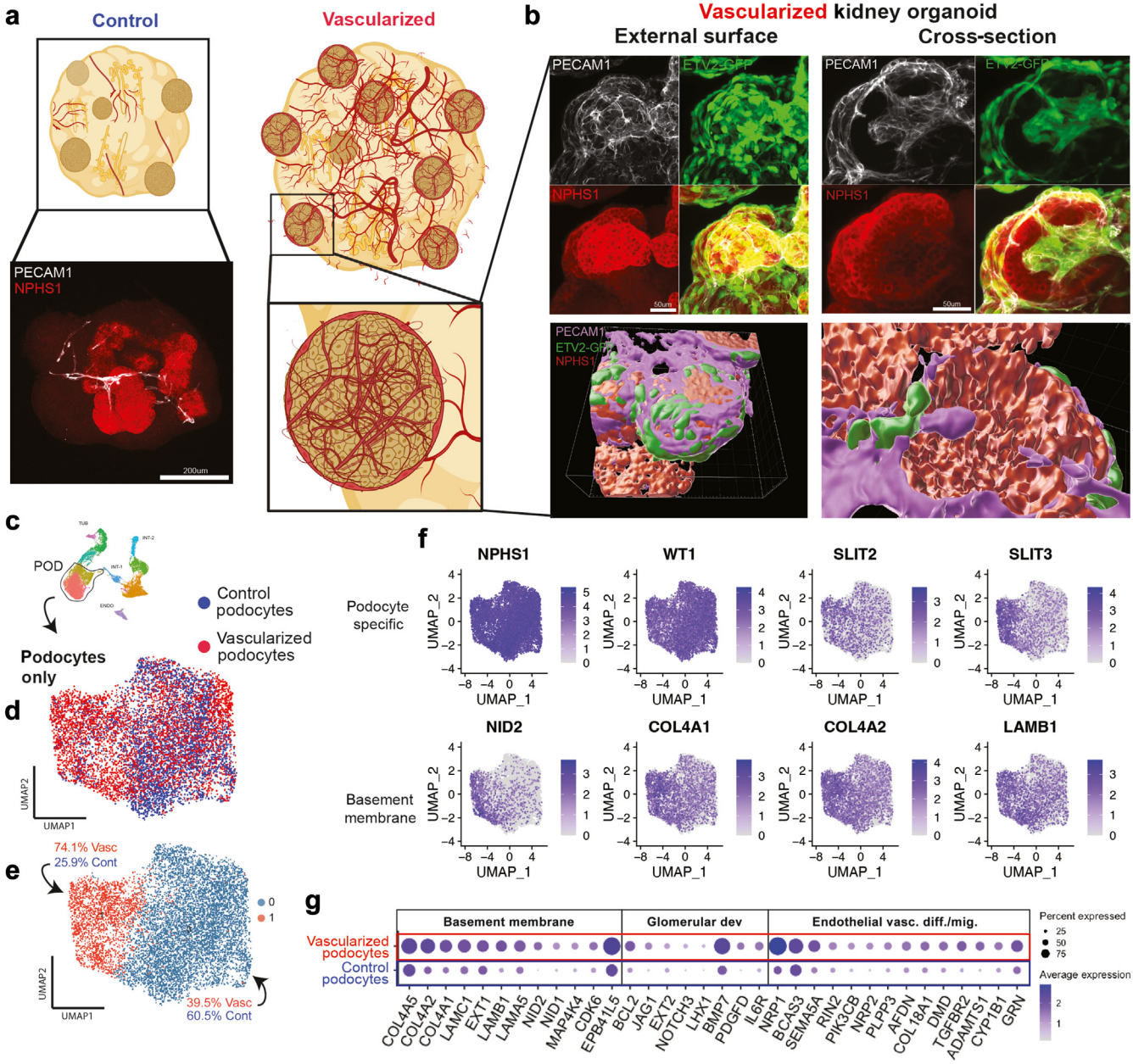

Figure 4 | Increased maturation of podocytes with vascularization. (**a**) Podocytes (POD) exist in nephrin (NPHS1^{+}) clusters in kidney organoids on the exterior surface by immunofluorescence. They become highly vascularized (vasc.) with the vascularization protocol and lack vascular integration with the control (cont) kidney organoid. Representative immunofluorescent images of 10 biological replicates. (**b**) Vascularized MANZ2-2 kidney organoids contain green fluorescent protein (GFP)$^{+}$ endothelial cells encasing the podocyte clusters from the external surface, and invaginating networks through the middle of the cluster. (**c**) Podocytes from both control and vascularized kidney organoid were (**d**) subclustered on uniform manifold approximation and projection (UMAP) for further analysis. (**e**) Podocytes distinctly cluster into 2 populations predominated largely by control or vascularized podocytes. (**f**) Podocyte-specific markers are present in both clusters, by feature plots; however, slit diaphragm and basement membrane markers are upregulated in cluster 0, predominated by vascularized podocytes. (**g**) Gene-set enrichment analysis identified upregulated pathways of basement membrane, glomerular development (dev), and endothelial vasculature differentiation (diff.) and migration (mig.) in the vascularized predominating podocyte cluster, with dot plots showing representative markers from each gene enrichment set ontology identifier. COL4A, collagen type IV alpha 2 chain; ETV2, ETS variant transcription factor 2; LAMB1, laminin subunit beta 1; NID2, nidogen 2; PECAM1, platelet and endothelial cell adhesion molecule 1; SLIT3, slit guidance ligand 3; WT1, Wilms' tumor protein 1. To optimize viewing of this image, please see the online version of this article at www.kidney-international.org.

analyzed using CellChat.[60] We found that vascularized kidney organoids had significantly higher *VEGF* pathway signaling between podocytes and endothelial cells, compared with that of the control kidney organoid (Supplementary Figure S22A). Despite control podocytes having a slightly higher level of *VEGFA* expression, vascularized podocytes

had a significantly higher percentage, and overall average expression, of endothelial *VEGFR1/VEGFR2* expression (Supplementary Figure S22B). These data demonstrate that the iETV2-hiPSCs endothelial niche within the vascularized kidney organoid promotes the emergence of a more mature podocyte population.

iETV2-hiPSC niche in vascularized organoid enables generation of a renin-positive interstitial cell population

The kidney interstitium is a heterogenous population[61–63] that contributes to the development, maturation, and structural support of other kidney parenchymal cell types.[64–66] To investigate the interstitial cell populations identified from the snRNAseq analysis, the interstitial cluster 1 cell population was reclustered on UMAP (Figure 5a). Interstitial cluster 1 was found to contain 7 subclusters, comprised of vascular smooth muscle renin$^+$ cells, 2 fibroblast populations (FIB-1 and FIB-2), proliferating fibroblast cells, mural cells, myofibroblasts, and proliferating myofibroblasts (Figure 5b). Cell type–specific markers of these clusters were aligned with previously published work identifying interstitial heterogeneity[67,68] (Figure 5c; Supplementary Figure S23A and B).

Contained within the *in vivo* kidney's interstitial population is a group of cells known as the juxtaglomerular apparatus, which contains renin-positive cells.[69] In addition to regulating blood pressure, renin also plays a critical role in the development of the kidney,[70] regulating proper vascular branching, arterial morphogenesis,[71,72] and tubular morphogenesis.[73] Some studies[74–76] have demonstrated organoid expression of *REN* by quantitative polymerase chain reaction and immunofluorescence, which can be increased with forskolin drug stimulation. However, the spatial localization of renin$^+$ cells and the development of these cells in relation to the endothelial lineage have not been examined closely. Our scRNAseq analysis identified the emergence of renin$^+$ cells in vascularized kidney organoids, without the need for exogenous stimuli such as forskolin or other additives to the culture media (Figure 5d and e). An interesting finding is that these cells were EGFP-negative, despite having arisen in the vascularized kidney organoid, indicating that they did not originate from the iETV2-hiPSC line (Supplementary Figure S24A). Renin$^+$ cells were identified by immunofluorescence in only the vascularized kidney organoids (Figure 5f–h), and a subset were double positive for the stromal marker platelet-derived growth factor receptor beta (PDGFRβ; Supplementary Figure S24B and C). Renin$^+$ cells localize adjacent to the podocyte clusters, and abut the endothelial cells, but they do not colabel with NPHS1 or PECAM1 (Figure 5g and h; Supplementary Figure S24D). No similar renin$^+$ cells are seen in the scRNAseq datasets from the Morizane and Takasato protocols (Supplementary Figure S25A). We compared our *REN*$^+$ cells gene expression to renin cells of P0 and adult mice[77] and found that the *REN*$^+$ cells of the vascularized kidney organoids tend to express more of the P0-specific markers, such as periostin (POSTN), CXC motif chemokine ligand 12 (CXCL12), bone morphogenetic protein 5 (BMP5), and roundabout guidance receptor 1 (ROBO1; Supplementary Figure S25B). Overall, we demonstrate that the incorporation of the iETV2-hiPSC endothelial niche enables the formation of a P0-like population of renin cells without the need for additional exogenous stimulation.

Forskolin can be used to trigger the release of renin in kidney organoid stromal cells.[74,78] Basal levels of *REN* expression in the vascularized kidney organoids are similar to *REN* levels in control MANZ2-2 kidney organoids that are stimulated with 10-mM forskolin. Stimulation of vascularized kidney organoids with 10-mM forskolin induced an ∼10-fold increase in *REN* expression relative to unstimulated vascularized kidney organoids (Figure 5i; Supplementary Figure S26A). This trend also is observed for human renin protein secreted into the supernatant of the organoid culture (Supplementary Figure S26B). Studies have shown that forskolin triggers tubular swelling in control organoids through cyclic adenosine monophosphate (cAMP) activation.[40] Consistent with this finding, we observed the cyst formation that occurs with forskolin stimulation, and we found this to be more pronounced in vascularized kidney organoids, compared to that in nonvascularized controls (Supplementary Figure S26C). This effect may reflect a role of endothelial cells in promoting electrophysiological ion transport.[79] These data demonstrate that the iETV2-hiPSCs endothelial niche induces a functional renin cell population without the need for exogenous stimulation, and provide a critical step forward in being able to model microphysiological systems of renin regulation.

Codeveloping iETV2-hiPSCs produce kidney-specific endothelial subtypes within kidney organoid

Previous studies have demonstrated both crosstalk between endothelial and epithelial cells in the kidney and the necessity of this crosstalk for proper codevelopment and maturation.[1,7,57,80] Furthermore, kidney endothelial populations contain distinct phenotypic and transcriptomic profiles.[81] To understand whether iETV2-hiPSCs mature and adopt an organ-specific fate, we reclustered the snRNAseq endothelial cell populations from control and vascularized kidney organoids (Figure 6a). Endothelial cells of the control and vascularized kidney organoids clustered into 3 distinct cell populations (Figure 6b). All endothelial cells from control and vascularized kidney organoids expressed endothelial markers, such as *PECAM1* and cadherin 5 (*CDH5*; Figure 6c). Using published markers of endothelial subtypes,[28,58,81] we determined that the clusters corresponded to glomerular-like (*PLAT*, *TBX3*, *SEMA5A*, *MAPT*, *EHD3*, *GATA5*), arterial-like (*GJA4*, *UNC4B*, *DEPP1*, *CXCR4*), and venous-like (*EPHB4*, *NR2F2*) endothelial populations (Figure 6d; Supplementary Figure S27). An interesting point to note is that endothelial cells from the control kidney organoids were present in only the arterial-like endothelial cluster (Figure 6d). The endothelial populations of the kidney organoids were compared to organ-specific endothelia of Tabula Sapiens using SingleCellNet. We found that the iETV2-hiPSC population gained a kidney-specific endothelial profile when incorporated into the

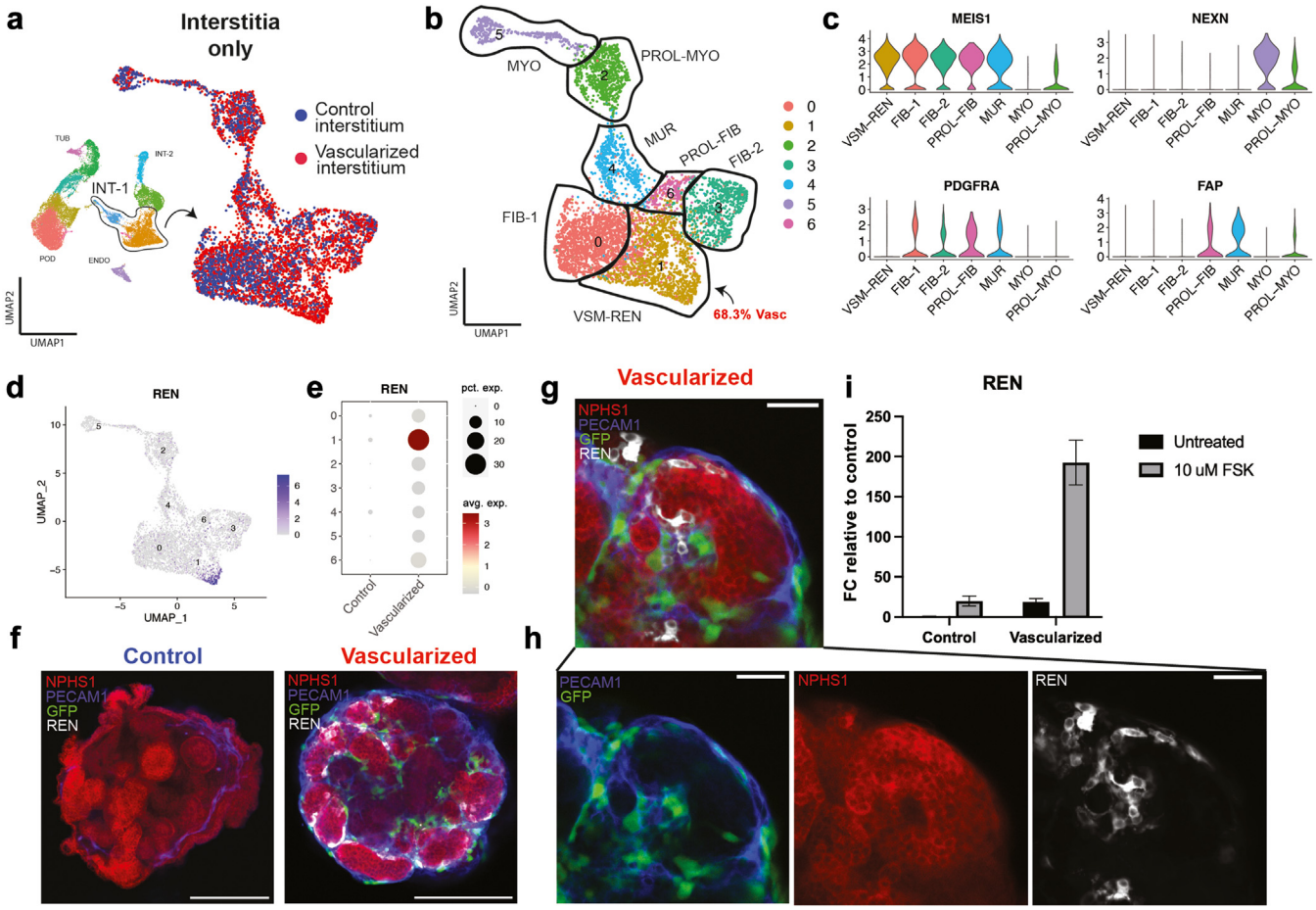

Figure 5 | Vascularization of kidney organoid enables emergence of a renin (REN) cell population. (**a**) Interstitial (INT) cells from MANZ2-2 control and vascularized kidney organoid were further analyzed in separate uniform manifold approximation and projections (UMAPs). (**b**) Interstitial cells clustered into 8 distinct populations. FIB-X, fibroblast-X; MYO, myoblast; MUR, mural; PROL-FIB, proliferative fibroblast; PROL-MYO, proliferative myoblast; VSM-REN, vascular smooth muscle renin. (**c**) Violin plots of key genes per cluster. (**d**) REN specifically localized to a population of cells on a feature plot that (**e**) originated largely from the vascularized kidney organoid as demonstrated on dot plot. (**f**) Control kidney organoid contains no REN^{+} cells on immunofluorescence, whereas vascularized kidney organoid contains many, spread across podocyte (nephrin [NPHS1]$^{+}$) clusters; bar = 200 mm. (**g**) Vascularized kidney organoid podocyte clusters contain REN^{+} cells within the cluster, (**h**) juxtaposing but not colabelling with NPHS1^{+} podocytes or green fluorescent protein (GFP)$^{+}$ platelet and endothelial cell adhesion molecule 1 (PECAM1)$^{+}$ endothelial cells; bar = 50 mm. (**i**) 10-uM forskolin (FSK)—a pro–renin stimulatory drug—supplemented in organoid media enables a 200-fold increase in renin expression in the vascularized kidney organoid by reverse transcription quantitative polymerase chain reaction (RT-qPCR). avg. exp, average expressed; ENDO, endothelial; FAP, fibroblast activation protein alpha; FC, fold change; FIB, fibroblast; MEIS1, Meis homeobox 1; MYO, myoblast; NEXN, nexilin F-actin binding protein; pct. exp., percentage expressed; PDGFRA, platelet-derived growth factor receptor alpha; TUB, tubular; VSM, vascular smooth muscle. To optimize viewing of this image, please see the online version of this article at www.kidney-international.org.

kidney organoid protocol, a contrast to the lack of specificity found in the iETV2-hiPSC monolayer. The glomerular-, arterial-, and venous-like cells were all classified in >50% with kidney-specific identification (Figure 6e).

These data demonstrate that the *ETV2*-induced organoid endothelial cells adopt an organ-specific maturity in codevelopment with the kidney organoid. By using the SEM, we identified that the endothelial cells on the external surface of the kidney organoid display a fenestrated cell membrane (Figure 6f). Additionally, endothelial cells of the vascularized kidney organoids contain a high level of expression of plasmalemma vehicle-associated protein (*PLVAP*), a marker of fenestrated endothelial cells associated with bridging diaphragms of fenestrae and caveolae[81] (Figure 6g). Our data demonstrate that the iETV2-hiPSCs are receptive to microenvironment cues of developing kidney organoids, and the resulting endothelial network yields a kidney-specific endothelial vascular tree alongside more-mature epithelial cells. Given that fenestrations play a critical role in glomerular filtration, this finding represents a significant novel advancement for the kidney-organoid field.[82]

DISCUSSION

Endothelial niches play a central role during organogenesis, controlling fate maturation, patterning, and morphogenetics events.[1–6] However, iPSC-derived organoids grown *in vitro* frequently lack a well-developed endothelial niche. The failure

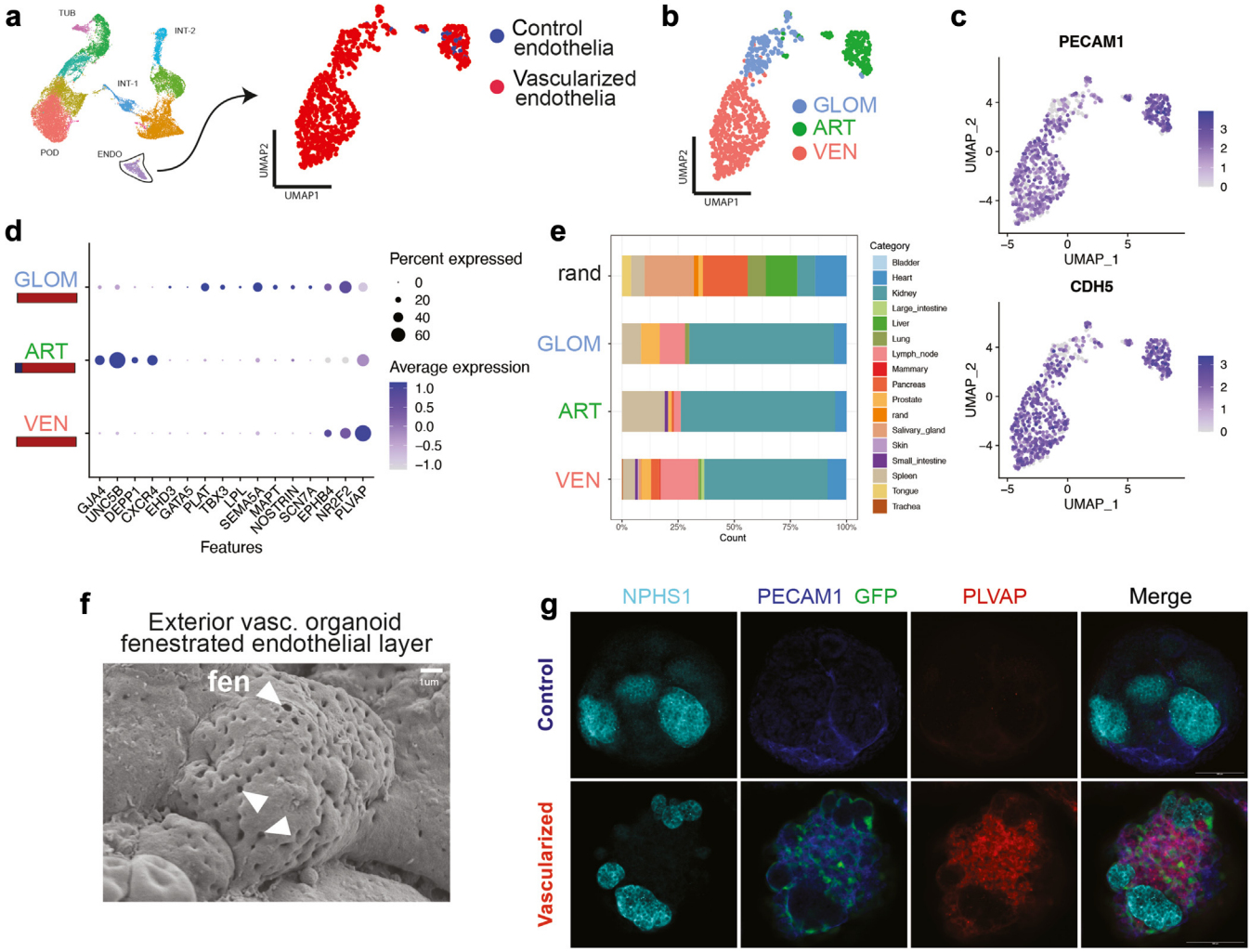

Figure 6 | Genetically inducible ETV2 human induced pluripotent stem cells (iETV2-hiPSCs) undergo maturation and organ specification. (**a**) Endothelial (ENDO) population of MANZ2-2 control and vascularized (vasc.) kidney organoids reclustered on uniform manifold approximation and projection (UMAP). (**b**) Endothelial cells subcluster into 3 distinct identities. (**c**) Endothelial cells are + platelet and endothelial cell adhesion molecule 1 (PECAM1)$^{+}$ cadherin 5 (CDH5)$^{+}$ on feature plot. (**d**) By dot plot, each distinct cluster represents glomerular (GLOM)-, arterial (ART)-, and venous (VEN)-like subidentity by canonical markers previously published. (**e**) SingleCellNet (Cahan Lab) classification of each subendothelial cell type using the Tabula Sapiens organ-specific endothelial dataset demonstrates kidney specification of endothelial cells. (**f**) On scanning electron microscopy, endothelial cell surface of vascularized kidney organoid demonstrates equally spaced fenestrations (fen); bar = 1 um. (**g**) Vascularized kidney organoid with iETV2-hiPSC express fenestration marker *PLVAP* on immunofluorescence; bar = 100 um. GFP, green fluorescent protein; INT, interstitial; PLVAP, plasmalemma vesicle-associated protein; POD, podocyte; rand, random; TUB, tubular. To optimize viewing of this image, please see the online version of this article at www.kidney-international.org.

to identify a common culture medium that can support the development of both resident parenchymal epithelia and endothelial populations has complicated this effort. Our strategy took advantage of ETV2, a "pioneer" transcription factor that promotes an endothelial fate,[13,14,83,84] to genetically engineer a doxycycline-inducible endothelial niche. We achieved this result by mixing a ratio of iETV2-hiPSCs to nontransgenic hiPSCs, allowing endothelial cell numbers to be "tuned" to a physiologically relevant quantity, while not overwhelming the organoid with vasculature. The resulting engineered niche is orthogonal to the organ-specific developmental program, but it operates in tandem, offering an innovative approach to vascularizing organoids.

We show for the first time in a kidney organoid model, that endothelial cells generated from iETV2-hiPSCs develop a fenestrated, endothelial network capable of morphologically integrating with tubular cells, podocytes, and interstitial cells in 3 dimensions. This vascularization leads to a podocyte population with encasing and invaginating endothelial cells that show a more mature transcriptional phenotype, and a more developed GBM. The vascularized kidney organoids also enable the emergence of an integrated, and responsive, renin cell population within the interstitium. Finally, we demonstrated that the development and maturation of these epithelial cells also coincides with the formation of a kidney-specific endothelial population,

demonstrating the potential codevelopment and crosstalk occurring between the epithelial, interstitial, and endothelial cells in generating a heterogenous maturing organoid. We observed a slightly diminished proportion of tubular cells in the vascularized kidney organoid, particularly distal tubule cells. Low *et al.*[28] have demonstrated the ability to modulate percentages of distinct cell types with dynamic modulation of WNT signaling via CHIR99021 exposure. Therefore, further regulation of the cell-type composition may be possible with the manipulation of exogenous factors present in the current protocol.

Endothelial cells are known to signal to surrounding tissues to drive differentiation.[85] Our vascularized organoids display glomeruli-like structures, comprised of juxtaposed podocytes and endothelial cells, with evidence of GBM formation and podocyte maturation. The podocyte clusters appear to contain endothelial cells encasing the podocyte cluster, with occasional endothelial cells invaginating into the podocyte cluster itself. We have demonstrated that early on in the *in vitro* culture, the iETV2-hiPSCs exist as a distinct population, and that only later, from days 14–18, are iETV2-hiPSC endothelial cells observed within podocyte clusters. However, more studies tracking the migration and movement of iETV2-hiPSCs in relation to any potential lack of S-shaped body structures are necessary to understand whether the iETV2-hiPSCs follow the same pattern of glomerular vascularization as that seen *in vivo*.[86–89]

CellChat analysis of the vascularized kidney organoid snRNAseq data demonstrated an increase in VEGF signaling, compared to that in control kidney organoids. Despite control organoids having a higher level of VEGFA, the vascularized organoid contained endothelial cells with higher levels of VEGF and its receptor (VEGFR)1 and VEGFR2 expression. This finding is consistent with results of VEGF signaling studies,[90,91] which show that VEGFA persists through podocyte development, but it diminishes during maturation. As described,[77] an underexpression or overexpression of VEGFA can result in glomerular disease, and thus, communication between podocytes and endothelial cells is required to finely regulate the balance of VEGFA required for normal glomerular physiology.

The podocytes in our vascularized organoids express higher levels of podocyte maturation markers,[53,58] such as *PTPRO*, *NPHS2*, *COL1A2*, *COL4A5*, *LAMC1*, *LAMA5*, and *CCN2*, and they show strong collagen type IV, alpha 5 (COL4A5) staining within the podocyte cluster. Although we demonstrate that *COL4A5* expression is upregulated in the podocytes of the vascularized organoid, we do not observe significant upregulation of *COL4A3* or *COL4A4*, despite mature basement membrane largely comprising the tetramer of α3α4α5. This observation is consistent with other reports showing minimal *COL4A3* expression in organoid podocytes.[92] Comparison of the podocyte expression profiles of the Morizane and Takasato protocols also shows a lack of *COL4A3* expression. Further work remains to immunofluorescent-label collagen monomers, as has been done in other publications, to understand basement membrane composition in kidney organoids.[92] Future studies on the podocyte–endothelial interaction will be needed to determine if GBM isotype switching occurs in the vascularized organoids, as has been shown *in vivo*.[56,59] Despite these shortcomings, we found that the podocytes of the control and vascularized kidney organoid contained a higher level of expression of mature podocyte markers, such as *NPHS1*, *NPHS2*, and *PTPRO*, than human fetal kidney, from previously published work.[53] Future studies aim to compare organoid scRNAseq data to other human fetal kidney datasets,[58] and investigate more-detailed immunofluorescent analysis on maturity of kidney organoid podocytes relative to human fetal kidney samples.

Similar to other reports,[58] we found a higher level of expression of some early podocyte markers in our vascularized organoids, compared to the controls, indicating that optimization of the culture conditions and/or the state of endothelial maturation is needed to further improve endothelial–podocyte crosstalk. These markers have been shown to persist following long-term transplantation.[58] To further mature kidney organoid podocytes, a necessary step may be to direct the differentiation of ETV2-induced endothelial cells into distinct glomerular endothelial cell types. This result possibly could be achieved with the introduction of fluid flow, or alternatively, the identity of glomerular endothelial cells could be induced genetically, in an approach similar to our iETV2 strategy, conceivably by the inclusion of the transcription factors GATA5 and T-box 3 (TBX3) to drive this fate.[93]

Other publications have demonstrated the emergence of renin$^+$ cells in *in vitro* human kidney organoids,[74,75] through an adapted version of the Takasato protocol.[94] Our study represents a significant step forward in that, without the use of any additional exogenous factors in the Przepiorski protocol,[45] the iETV2-hiPSCs addition results in the emergence of renin$^+$ cells. Given the role renin cells play in the development of vasculature and overall kidney morphogenesis,[70–73] the ability of the iETV2-hiPSCs to be selectively added to or subtracted from a kidney organoid model can be utilized to parse the exact cell–cell communication that occurs during development of renin cells and endothelial cell networks during *in vitro* development. We demonstrate that the anatomic position of the renin$^+$ cells repeatably shows that the renin cells abut endothelial cells and podocytes, and colabel as platelet-derived growth factor receptor beta (PDGFRB). However, in future studies, we aim to understand whether the renin$^+$ cells interact with mesangial and distal convoluted tubules to form a rudimentary responsive juxtaglomerular apparatus. Furthermore, although we identify by scRNAseq populations of mural-like cells, a critical step in future work will be to identify the anatomic location of these and other vascular supporting endothelial cells relative to the kidney parenchyma.

During development, organs develop vascular networks with different types of vessels, including arteries, veins, and capillaries that are specialized to each particular organ.[81] The

Low *et al.* [28] study demonstrated the emergence of preliminary arterial and venous specification in kidney organoids on scRNAseq. Although our control kidney organoids also contained an arterial subspecialization, the vascularized kidney organoids contained 2 additional novel endothelial subtypes—glomerular- and venous-specific subpopulations of endothelial cells. Although these endothelial subtypes have been identified through examining scRNAseq expression patterns with literature-defined markers, we acknowledge the limitations in this method and that further work remains to both characterize the exact immunophenotypic profile of kidney endothelial subtypes[95] and further identify endothelial subtypes in the kidney organoid with immunofluorescent studies. Furthermore, additional subtypes of endothelial cells exist in the human *in vivo* kidney.[81] One reason for the lack of phenotypic diversity, akin to native kidney, may be that the organoids were grown under static conditions, whereas *in vivo*, the developing vasculature is highly responsive to blood flow, which helps remodel the immature plexus and induce different arteriovenous fates.[96,97] The addition of existing fluidic protocols to our current organoid protocol may achieve a more mature vascular network. Despite this possibility, the endothelial cells adopted a transcriptional signature that is similar to that of endogenous endothelia from the adult kidney. This finding suggests that the organoid microenvironment is providing differentiation signals to the vascular plexus. As the nature of these signals has not been well characterized, our vascularized organoids offer a tool to investigate these processes.

Overall, the human kidney organoids generated with the use of the inducible endothelial niche contain a vascular network that morphologically integrates with podocytes, interstitial cells, and renin cells in a way that will allow investigation of disease processes that are often determined on a histologic basis. Therefore, this study moves the field of kidney-tissue engineering a significant step forward toward more adequate modeling of diseases of GBM formation, disease of the juxtaglomerular apparatus, and with additional engineering modules—modeling of physiological conditions such as blood pressure and cyst formation. This inducible endothelial progenitor iPSC line was integrated easily into an established kidney organoid protocol, and thus, it demonstrates the potential for other organ systems and models to include an inducible vascular niche.[3,6,13–15,98,99] Our study lays groundwork for an easy to use and widely applicable engineering method for manipulation and augmentation of a tissue vascular niche during *in vitro* human kidney organogenesis.

DISCLOSURE

All the authors declared no competing interests.

DATA STATEMENT

The scRNAseq data of the control and vascularized kidney organoids presented in this study are openly available in GEO under accession number GSE232767. The scRNAseq data for comparisons made to Tabula Sapiens are publicly and openly available at https://tabula-sapiens-portal.ds.czbiohub.org/. The code used in the analyses of this work is available upon request to the corresponding authors.

ACKNOWLEDGMENTS

NAH reports receiving support for this research from the National Institute of Diabetes and Digestive and Kidney Diseases (NIDDK) UC2 DK126122 and U54 DK137329, the Department of Defense HT9425-23-1-0480, and from the Vascular Medicine Institute, the Hemophilia Center of Western Pennsylvania, and the Institute for Transfusion Medicine. MRE discloses support for publication of this work by the National Institutes of Health (NIH) center grant P30 DK120531 from the NIDDK (to Pittsburgh Liver Research Center [PLRC]); NIH grants R01 EB028532 from the National Institute of Biomedical Imaging and Bioengineering (NIBIB), R01 HL141805 from the National Heart Lung and Blood Institute, and NSF grant (award number 2134999) (to MRE). SK discloses support for publication of this work by NIH center grant P30 DK120531 from the NIDDK (to Pittsburgh Liver Research Center [PLRC]); and NIH grants R01 EB028532 and R01EB024562 from the NIBIB. JCM discloses support for the research of this work, in part, from the University of Pittsburgh CATER training grant T32EB001026. AW discloses support for the imaging and instrumentation from 1S10OD019973-01. SW discloses support for the imaging and instrumentation from 1S10OD016236-01. AP acknowledges the Ben J. Lipps Research Fellowship Program for their support. CC and TC acknowledge the NIH (R01DK127634, RC2 DK125960) and Cancer Prevention and Research Institute of Texas (RP220201) for supporting the research in this work. MHL and SH acknowledge the support of NIH DK107344. The authors thank Tracy Tabib, Heidi Monroe, and the team at the Single Cell Genomics Core of the University of Pittsburgh for performing scRNAseq and snRNAseq.

Supplementary material is available online at www.kidney-international.org.

REFERENCES

1. Ramasamy SK, Kusumbe AP, Adams RH. Regulation of tissue morphogenesis by endothelial cell-derived signals. *Trends Cell Biol*. 2015;25:148–157.
2. Lei Z, Hu X, Wu Y, et al. The role and mechanism of the vascular endothelial niche in diseases: a review. *Front Physiol*. 2022;13:863265.
3. Butler JM, Kobayashi H, Rafii S. Instructive role of the vascular niche in promoting tumour growth and tissue repair by angiocrine factors. *Nat Rev Cancer*. 2010;10:138–146.
4. Rafii S, Butler JM, Ding BS. Angiocrine functions of organ-specific endothelial cells. *Nature*. 2016;529:316–325.
5. Crivellato E, Nico B, Ribatti D. Contribution of endothelial cells to organogenesis: a modern reappraisal of an old Aristotelian concept. *J Anat*. 2007;211:415–427.
6. Ribatti D, Tamma R, Annese T. The role of vascular niche and endothelial cells in organogenesis and regeneration. *Exp Cell Res*. 2021;398:112398.
7. Azizoglu DB, Cleaver O. Blood vessel crosstalk during organogenesis—focus on pancreas and endothelial cells. *Wiley Interdiscip Rev Dev Biol*. 2016;5:598–617.
8. Kolesky DB, Homan KA, Skylar-Scott MA, Lewis JA. Three-dimensional bioprinting of thick vascularized tissues. *Proc Natl Acad Sci U S A*. 2016;113:3179–3184.
9. Zohar B, Blinder Y, Mooney DJ, Levenberg S. Flow-induced vascular network formation and maturation in three-dimensional engineered tissue. *ACS Biomater Sci Eng*. 2018;4:1265–1271.
10. Holloway EM, Wu JH, Czerwinski M, et al. Differentiation of human intestinal organoids with endogenous vascular endothelial cells. *Dev Cell*. 2020;54:516–528 e7.
11. Lange L, Hoffmann D, Schwarzer A, et al. Inducible forward programming of human pluripotent stem cells to hemato-endothelial progenitor cells with hematopoietic progenitor potential. *Stem Cell Reports*. 2020;14:122–137.

12. Zhang H, Yamaguchi T, Kawabata K. The maturation of iPS cell-derived brain microvascular endothelial cells by inducible-SOX18 expression. *Fluids Barriers CNS*. 2023;20:10.
13. Palikuqi B, Nguyen DT, Li G, et al. Adaptable haemodynamic endothelial cells for organogenesis and tumorigenesis. *Nature*. 2020;585:426–432.
14. Skylar-Scott MA, Huang JY, Lu A, et al. Orthogonally induced differentiation of stem cells for the programmatic patterning of vascularized organoids and bioprinted tissues. *Nat Biomed Eng*. 2022;6:449–462.
15. Cakir B, Xiang Y, Tanaka Y, et al. Engineering of human brain organoids with a functional vascular-like system. *Nat Methods*. 2019;16:1169–1175.
16. Jourde-Chiche N, Fakhouri F, Dou L, et al. Endothelium structure and function in kidney health and disease. *Nat Rev Nephrol*. 2019;15:87–108.
17. He J, Xu Y, Koya D, Kanasaki K. Role of the endothelial-to-mesenchymal transition in renal fibrosis of chronic kidney disease. *Clin Exp Nephrol*. 2013;17:488–497.
18. Miao C, Zhu X, Wei X, et al. Pro- and anti-fibrotic effects of vascular endothelial growth factor in chronic kidney diseases. *Ren Fail*. 2022;44:881–892.
19. Lebedenko CG, Banerjee IA. Enhancing kidney vasculature in tissue engineering—current trends and approaches: a review. *Biomimetics (Basel)*. 2021;6:40.
20. Homan KA, Gupta N, Kroll KT, et al. Flow-enhanced vascularization and maturation of kidney organoids *in vitro*. *Nat Methods*. 2019;16:255–262.
21. Lee HN, Choi YY, Kim JW, et al. Effect of biochemical and biomechanical factors on vascularization of kidney organoid-on-a-chip. *Nano Converg*. 2021;8:35.
22. Bas-Cristobal Menendez A, Du Z, van den Bosch TPP, et al. Creating a kidney organoid-vasculature interaction model using a novel organ-on-chip system. *Sci Rep*. 2022;12:20699.
23. Kim JW, Nam SA, Yi J, et al. Kidney decellularized extracellular matrix enhanced the vascularization and maturation of human kidney organoids. *Adv Sci (Weinh)*. 2022;9:e2103526.
24. Kolesky DB, Truby RL, Gladman AS, et al. 3D bioprinting of vascularized, heterogeneous cell-laden tissue constructs. *Adv Mater*. 2014;26:3124–3130.
25. van den Berg CW, Ritsma L, Avramut MC, et al. Renal subcapsular transplantation of PSC-derived kidney organoids induces neo-vasculogenesis and significant glomerular and tubular maturation *in vivo*. *Stem Cell Reports*. 2018;10:751–765.
26. Koning M, Dumas SJ, Avramut MC, et al. Vasculogenesis in kidney organoids upon transplantation. *NPJ Regen Med*. 2022;7:40.
27. Czerniecki SM, Cruz NM, Harder JL, et al. High-throughput screening enhances kidney organoid differentiation from human pluripotent stem cells and enables automated multidimensional phenotyping. *Cell Stem Cell*. 2018;22:929–940 e4.
28. Low JH, Li P, Chew EGY, et al. Generation of human PSC-derived kidney organoids with patterned nephron segments and a *de novo* vascular network. *Cell Stem Cell*. 2019;25:373–387 e9.
29. Ryan AR, England AR, Chaney CP, et al. Vascular deficiencies in renal organoids and *ex vivo* kidney organogenesis. *Dev Biol*. 2021;477:98–116.
30. Zhang H, Yamaguchi T, Kokubu Y, Kawabata K. Transient ETV2 expression promotes the generation of mature endothelial cells from human pluripotent stem cells. *Biol Pharm Bull*. 2022;45:483–490.
31. Morita R, Suzuki M, Kasahara H, et al. ETS transcription factor ETV2 directly converts human fibroblasts into functional endothelial cells. *Proc Natl Acad Sci U S A*. 2015;112:160–165.
32. Przepiorski A, Crunk AE, Holm TM, et al. A simplified method for generating kidney organoids from human pluripotent stem cells. *J Vis Exp*. 2021:(170):10.3791/62452.
33. Przepiorski A, Sander V, Tran T, et al. A simple bioreactor-based method to generate kidney organoids from pluripotent stem cells. *Stem Cell Reports*. 2018;11:470–484.
34. Guye P, Ebrahimkhani MR, Kipniss N, et al. Genetically engineering self-organization of human pluripotent stem cells into a liver bud-like tissue using Gata6. *Nat Commun*. 2016;7:10243.
35. Zhou M, Ni J, Huang P, Liu X. Generation of a doxycycline-inducible ETV2 expression cell line using PiggyBac transposase system. *Stem Cell Res*. 2023;66:102985.
36. Velazquez JJ, LeGraw R, Moghadam F, et al. Gene regulatory network analysis and engineering directs development and vascularization of multilineage human liver organoids. *Cell Syst*. 2021;12:41–55 e11.
37. Oh JK, Przepiorski A, Chang H, et al. Derivation of induced pluripotent stem cell lines from New Zealand donors. *J R Soc N Z*. 2020;52:54–67.
38. Susaki EA, Tainaka K, Perrin D, et al. Advanced CUBIC protocols for whole-brain and whole-body clearing and imaging. *Nat Protoc*. 2015;10:1709–1727.
39. Matsumoto K, Mitani TT, Horiguchi SA, et al. Advanced CUBIC tissue clearing for whole-organ cell profiling. *Nat Protoc*. 2019;14:3506–3537.
40. Muntifering M, Castranova D, Gibson GA, et al. Clearing for deep tissue imaging. *Curr Protoc Cytom*. 2018;86:e38.
41. Trapnell C, Cacchiarelli D, Grimsby J, et al. The dynamics and regulators of cell fate decisions are revealed by pseudotemporal ordering of single cells. *Nat Biotechnol*. 2014;32:381–386.
42. Qiu X, Mao Q, Tang Y, et al. Reversed graph embedding resolves complex single-cell trajectories. *Nat Methods*. 2017;14:979–982.
43. Tabula Sapiens C, Jones RC, Karkanias J, et al. The Tabula Sapiens: a multiple-organ, single-cell transcriptomic atlas of humans. *Science*. 2022;376:eabl4896.
44. Tan Y, Cahan P. SingleCellNet: a computational tool to classify single cell RNA-Seq data across platforms and across species. *Cell Syst*. 2019;9:207–213 e2.
45. Sander V, Przepiorski A, Crunk AE, et al. Protocol for large-scale production of kidney organoids from human pluripotent stem cells. *STAR Protoc*. 2020;1:100150.
46. Przepiorski A, Vanichapol T, Espiritu EB, et al. Modeling oxidative injury response in human kidney organoids. *Stem Cell Res Ther*. 2022;13:76.
47. Zudaire E, Gambardella L, Kurcz C, Vermeren S. A computational tool for quantitative analysis of vascular networks. *PLoS One*. 2011;6:e27385.
48. Wilson SB, Howden SE, Vanslambrouck JM, et al. DevKidCC allows for robust classification and direct comparisons of kidney organoid datasets. *Genome Med*. 2022;14:19.
49. Combes AN, Zappia L, Er PX, et al. Single-cell analysis reveals congruence between kidney organoids and human fetal kidney. *Genome Med*. 2019;11:3.
50. Morizane R, Bonventre JV. Generation of nephron progenitor cells and kidney organoids from human pluripotent stem cells. *Nat Protoc*. 2017;12:195–207.
51. Morizane R, Lam AQ, Freedman BS, et al. Nephron organoids derived from human pluripotent stem cells model kidney development and injury. *Nat Biotechnol*. 2015;33:1193–1200.
52. Wu H, Uchimura K, Donnelly EL, et al. Comparative analysis and refinement of human PSC-derived kidney organoid differentiation with single-cell transcriptomics. *Cell Stem Cell*. 2018;23:869–881.e8.
53. Hochane M, van den Berg PR, Fan X, et al. Single-cell transcriptomics reveals gene expression dynamics of human fetal kidney development. *PLoS Biol*. 2019;17:e3000152.
54. Suh JH, Miner JH. The glomerular basement membrane as a barrier to albumin. *Nat Rev Nephrol*. 2013;9:470–477.
55. Wiggins RC. The spectrum of podocytopathies: a unifying view of glomerular diseases. *Kidney Int*. 2007;71:1205–1214.
56. Hale LJ, Howden SE, Phipson B, et al. 3D organoid-derived human glomeruli for personalised podocyte disease modelling and drug screening. *Nat Commun*. 2018;9:5167.
57. Daniel E, Cleaver O. Vascularizing organogenesis: lessons from developmental biology and implications for regenerative medicine. *Curr Top Dev Biol*. 2019;132:177–220.
58. Tran T, Lindstrom NO, Ransick A, et al. *In vivo* developmental trajectories of human podocyte inform *in vitro* differentiation of pluripotent stem cell-derived podocytes. *Dev Cell*. 2019;50:102–116.e6.
59. Abrahamson DR. Role of the podocyte (and glomerular endothelium) in building the GBM. *Semin Nephrol*. 2012;32:342–349.
60. Jin S, Guerrero-Juarez CF, Zhang L, et al. Inference and analysis of cell-cell communication using CellChat. *Nat Commun*. 2021;12:1088.
61. Nishinakamura R. Human kidney organoids: progress and remaining challenges. *Nat Rev Nephrol*. 2019;15:613–624.
62. Lindstrom NO, Guo J, Kim AD, et al. Conserved and divergent features of mesenchymal progenitor cell types within the cortical nephrogenic niche of the human and mouse kidney. *J Am Soc Nephrol*. 2018;29:806–824.
63. Combes AN, Phipson B, Lawlor KT, et al. Single cell analysis of the developing mouse kidney provides deeper insight into marker gene expression and ligand-receptor crosstalk. *Development*. 2019;146(dev):178673.
64. Mao Y, Francis-West P, Irvine KD. Fat4/Dchs1 signaling between stromal and cap mesenchyme cells influences nephrogenesis and ureteric bud branching. *Development*. 2015;142:2574–2585.

65. Bagherie-Lachidan M, Reginensi A, Pan Q, et al. Stromal Fat4 acts non-autonomously with Dchs1/2 to restrict the nephron progenitor pool. *Development*. 2015;142:2564–2573.
66. Das A, Tanigawa S, Karner CM, et al. Stromal-epithelial crosstalk regulates kidney progenitor cell differentiation. *Nat Cell Biol*. 2013;15:1035–1044.
67. England AR, Chaney CP, Das A, et al. Identification and characterization of cellular heterogeneity within the developing renal interstitium. *Development*. 2020;147(dev):190108.
68. Kirita Y, Wu H, Uchimura K, et al. Cell profiling of mouse acute kidney injury reveals conserved cellular responses to injury. *Proc Natl Acad Sci U S A*. 2020;117:15874–15883.
69. Castrop H, Hocherl K, Kurtz A, et al. Physiology of kidney renin. *Physiol Rev*. 2010;90:607–673.
70. Takahashi N, Lopez ML, Cowhig JE Jr, et al. Ren1c homozygous null mice are hypotensive and polyuric, but heterozygotes are indistinguishable from wild-type. *J Am Soc Nephrol*. 2005;16:125–132.
71. Gomez RA, Lynch KR, Sturgill BC, et al. Distribution of renin mRNA and its protein in the developing kidney. *Am J Physiol*. 1989;257:F850–E858.
72. Reddi V, Zaglul A, Pentz ES, Gomez RA. Renin-expressing cells are associated with branching of the developing kidney vasculature. *J Am Soc Nephrol*. 1998;9:63–71.
73. Sequeira-Lopez ML, Nagalakshmi VK, Li M, et al. Vascular versus tubular renin: role in kidney development. *Am J Physiol Regul Integr Comp Physiol*. 2015;309:R650–R657.
74. Shankar AS, Du Z, Mora HT, et al. Human kidney organoids produce functional renin. *Kidney Int*. 2021;99:134–147.
75. Yanofsky SM, Dugas CM, Katsurada A, et al. Angiotensin II biphasically regulates cell differentiation in human iPSC-derived kidney organoids. *Am J Physiol Renal Physiol*. 2021;321:F559–F571.
76. Tsujimoto H, Hoshina A, Mae SI, et al. Selective induction of human renal interstitial progenitor-like cell lineages from iPSCs reveals development of mesangial and EPO-producing cells. *Cell Rep*. 2024;43:113602.
77. Brunskill EW, Sequeira-Lopez ML, Pentz ES, et al. Genes that confer the identity of the renin cell. *J Am Soc Nephrol*. 2011;22:2213–2225.
78. Trush O, Takasato M. Kidney organoid research: current status and applications. *Curr Opin Genet Dev*. 2022;75:101944.
79. Freedman BS. Physiology assays in human kidney organoids. *Am J Physiol Renal Physiol*. 2022;322:F625–F638.
80. Del Moral PM, Sala FG, Tefft D, et al. VEGF-A signaling through Flk-1 is a critical facilitator of early embryonic lung epithelial to endothelial crosstalk and branching morphogenesis. *Dev Biol*. 2006;290:177–188.
81. Dumas SJ, Meta E, Borri M, et al. Phenotypic diversity and metabolic specialization of renal endothelial cells. *Nat Rev Nephrol*. 2021;17:441–464.
82. Satchell SC, Braet F. Glomerular endothelial cell fenestrations: an integral component of the glomerular filtration barrier. *Am J Physiol Renal Physiol*. 2009;296:F947–F956.
83. Ginsberg M, James D, Ding BS, et al. Efficient direct reprogramming of mature amniotic cells into endothelial cells by ETS factors and TGFbeta suppression. *Cell*. 2012;151:559–575.
84. Gomez-Salinero JM, Itkin T, Rafii S. Developmental angiocrine diversification of endothelial cells for organotypic regeneration. *Dev Cell*. 2021;56:3042–3051.
85. Dimke H, Sparks MA, Thomson BR, et al. Tubulovascular cross-talk by vascular endothelial growth factor a maintains peritubular microvasculature in kidney. *J Am Soc Nephrol*. 2015;26:1027–1038.
86. Abrahamson DR, Robert B, Hyink DP, et al. Origins and formation of microvasculature in the developing kidney. *Kidney Int Suppl*. 1998;67:S7–S11.
87. Stolz DB, Sims-Lucas S. Unwrapping the origins and roles of the renal endothelium. *Pediatr Nephrol*. 2015;30:865–872.
88. Abrahamson DR. Development of kidney glomerular endothelial cells and their role in basement membrane assembly. *Organogenesis*. 2009;5:275–287.
89. Robert B, St John PL, Hyink DP, Abrahamson DR. Evidence that embryonic kidney cells expressing flk-1 are intrinsic, vasculogenic angioblasts. *Am J Physiol*. 1996;271:F744–F753.
90. Eremina V, Baelde HJ, Quaggin SE. Role of the VEGF–a signaling pathway in the glomerulus: evidence for crosstalk between components of the glomerular filtration barrier. *Nephron Physiol*. 2007;106:p32–p37.
91. Eremina V, Quaggin SE. The role of VEGF-A in glomerular development and function. *Curr Opin Nephrol Hypertens*. 2004;13:9–15.
92. Jansen J, van den Berge BT, van den Broek M, et al. Human pluripotent stem cell-derived kidney organoids for personalized congenital and idiopathic nephrotic syndrome modeling. *Development*. 2022;149(dev):200198.
93. Barry DM, McMillan EA, Kunar B, et al. Molecular determinants of nephron vascular specialization in the kidney. *Nat Commun*. 2019;10:5705.
94. Takasato M, Er PX, Chiu HS, Little MH. Generation of kidney organoids from human pluripotent stem cells. *Nat Protoc*. 2016;11:1681–1692.
95. Daniel E, Azizoglu DB, Ryan AR, et al. Spatiotemporal heterogeneity and patterning of developing renal blood vessels. *Angiogenesis*. 2018;21:617–634.
96. le Noble F, Moyon D, Pardanaud L, et al. Flow regulates arterial-venous differentiation in the chick embryo yolk sac. *Development*. 2004;131:361–375.
97. Wang H, Riha GM, Yan S, et al. Shear stress induces endothelial differentiation from a murine embryonic mesenchymal progenitor cell line. *Arterioscler Thromb Vasc Biol*. 2005;25:1817–1823.
98. Vargas-Valderrama A, Messina A, Mitjavila-Garcia MT, Guenou H. The endothelium, a key actor in organ development and hPSC-derived organoid vascularization. *J Biomed Sci*. 2020;27:67.
99. Gori JL, Butler JM, Chan YY, et al. Vascular niche promotes hematopoietic multipotent progenitor formation from pluripotent stem cells. *J Clin Invest*. 2015;125:1243–1254.